ARL-CR-0853 ● JULY 2020

DEVCOM ARMY RESEARCH LABORATORY

The Addition of Cohesive Wedge Elements into the Elastic Plastic Impact Computation (EPIC) Code

prepared by Charles A Gerlach and Timothy J Holmquist
Southwest Research Institute
5353 Wayzata Boulevard, Suite 607
Minneapolis, MN 55416

under contract W911QX-17-D-0014-0002

NOTICES

Disclaimers

The findings in this report are not to be construed as an official Department of the Army position unless so designated by other authorized documents.

Citation of manufacturer's or trade names does not constitute an official endorsement or approval of the use thereof.

Destroy this report when it is no longer needed. Do not return it to the originator.

ARL-CR-0853 ● JULY 2020

The Addition of Cohesive Wedge Elements into the Elastic Plastic Impact Computation (EPIC) Code

prepared by Charles A Gerlach and Timothy J Holmquist
Southwest Research Institute
5353 Wayzata Boulevard, Suite 607
Minneapolis, MN 55416

under contract W911QX-17-D-0014-0002

REPORT DOCUMENTATION PAGE

Form Approved

OMB No. 0704-0188

1. REPORT DATE *(DD-MM-YYYY)*	**2. REPORT TYPE**	**3. DATES COVERED (From - To)**
July 2020	Contractor Report	October 2017–January 2018

4. TITLE AND SUBTITLE

The Addition of Cohesive Wedge Elements into the Elastic Plastic Impact Computation (EPIC) Code

5a. CONTRACT NUMBER

W911QX-17-D-0014-0002

5b. GRANT NUMBER

5c. PROGRAM ELEMENT NUMBER

6. AUTHOR(S)

Charles A Gerlach and Timothy J Holmquist

5d. PROJECT NUMBER

18.23292

5e. TASK NUMBER

5f. WORK UNIT NUMBER

7. PERFORMING ORGANIZATION NAME(S) AND ADDRESS(ES)

Southwest Research Institute
Engineering Dynamics Department
5353 Wayzata Blvd.
Minneapolis, MN 55416

8. PERFORMING ORGANIZATION REPORT NUMBER

9. SPONSORING/MONITORING AGENCY NAME(S) AND ADDRESS(ES)

CCDC Army Research Laboratory
ATTN: FCDD-RLW-B
Aberdeen Proving Ground, MD 21005

10. SPONSOR/MONITOR'S ACRONYM(S)

11. SPONSOR/MONITOR'S REPORT NUMBER(S)

ARL-CR-0853

12. DISTRIBUTION/AVAILABILITY STATEMENT

Approved for public release: distribution unlimited

13. SUPPLEMENTARY NOTES

14. ABSTRACT

This report documents the addition of cohesive wedge elements into the 2017 beta version of the Elastic Plastic Impact Computation (EPIC) code. These elements allow the attachment of triangular-faced tetrahedral elements. This new capability allows symmetric brick elements (24 tetrahedral elements arranged in a hexahedron) to be attached to other symmetric brick elements using one layer of cohesive wedge elements. The cohesive wedge elements use the cohesive material model (implemented previously by Beissel) to simulate bond strength. The advantage of using cohesive elements, instead of solid elements, is that very thin layers can be used without affecting the time increment.

15. SUBJECT TERMS

cohesive element, wedge, EPIC2017 Beta, bond strength, triangular-faced, Elastic Plastic Impact Computation

16. SECURITY CLASSIFICATION OF:			**17. LIMITATION OF ABSTRACT**	**18. NUMBER OF PAGES**	**19a. NAME OF RESPONSIBLE PERSON**
a. REPORT	**b. ABSTRACT**	**c. THIS PAGE**			Andrew Tonge
Unclassified	Unclassified	Unclassified	UU	20	**19b. TELEPHONE NUMBER (Include area code)** 410-278-1069

Contents

List of Figures

List of Tables

Preface

This work was performed for the US Army Combat Capabilities Development Command Army Research Laboratory under contract W911QX-17-D-0014-0002. The authors would like to thank Stephen Beissel (Southwest Research Institute) for his contributions to this work.

Summary

This report documents the addition of cohesive wedge elements into the 2017 beta version of the Elastic Plastic Impact Computation (EPIC) code.[1] These elements allow the attachment of triangular-faced tetrahedral elements. This new capability allows symmetric brick elements (24 tetrahedral elements arranged in a hexahedron) to be attached to other symmetric brick elements using one layer of cohesive wedge elements. The cohesive wedge elements use the cohesive material model implemented previously by Beissel[2] to simulate bond strength. The advantage of using cohesive elements, instead of solid elements, is that very thin layers can be used without affecting the time increment.

[1]Johnson GR, Beissel SR, Gerlach CA, Holmquist TJ. User instructions for the 2017 beta version of the EPIC code. San Antonio (TX): Southwest Research Institute; 2017 Dec.
[2]Beissel SR. The addition of a cohesive model to the EPIC code for simulating interfaces in composite materials. San Antonio (TX): Southwest Research Institute; 2016 Aug. Report No.: 18.19018/017.

1. Introduction

In the fabrication of armor, components are often attached together using adhesives, and it is of interest to know how this "bonding layer" affects armor performance. Modeling adhesive layers using solid elements is generally not feasible because these layers are typically very thin, requiring a very small time increment and very long computing times. In 2016 Beissel implemented cohesive hexahedral elements, and a cohesive material model, into the Elastic Plastic Impact Computation (EPIC) code.[1] This allowed for solid hexahedral elements to be attached to other solid hexahedral elements using one layer of cohesive hexahedral elements. The cohesive elements are used to represent the adhesive between two joined materials and the cohesive material model is used to describe the adhesive strength. The advantage of using cohesive elements, instead of solid elements, is that very thin cohesive elements can be used without affecting the time increment. Beissel used these elements to successfully model the bonding and delamination of metal plates subjected to sphere impact, but the deformations were relatively small.

The US Army Combat Capabilities Development Command (CCDC) Army Research Laboratory (ARL) recently identified a lack of robustness when these elements were subjected to large deformations resulting from projectile impact and perforation.[2] Because of this limitation, the CCDC Army Research Laboratory provided funding to develop cohesive wedge elements to attach symmetric brick elements (24 tetrahedral elements in a hexahedron). Symmetric brick elements have been shown to be very robust for severe distortions. The remainder of this report presents an overview of how to use cohesive wedge elements in EPIC, and some example computations to verify that they are behaving as intended.

2. Using Cohesive Wedge Elements in EPIC

Figure 1 presents the geometry of a single wedge element and four wedge elements arranged in a hexahedron. This four-wedge arrangement is used to attach two symmetric bricks. A new feature developed under this effort allows a plate, comprising four wedge elements, to be generated with the EPIC plate generator. The wedge element becomes a cohesive wedge element when its response is defined by the cohesive material model, implemented in 2016.[1] The cohesive material model is simple and efficient, and requires only five constants. Figure 2 presents a schematic of the cohesive strength model and the EPIC input required to define it.

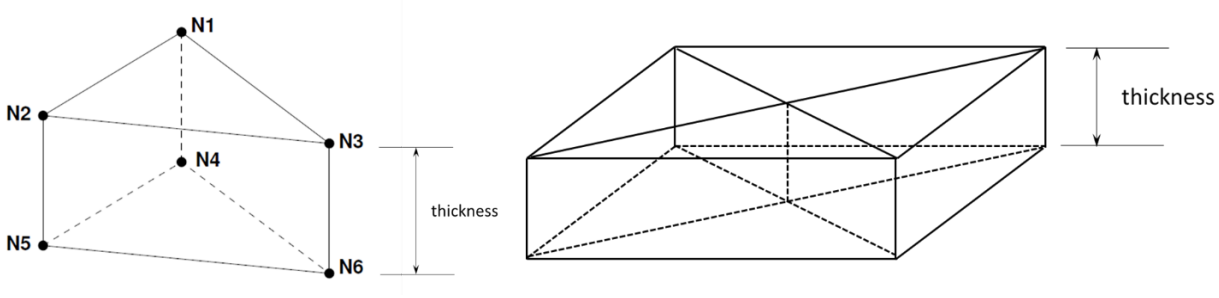

Fig. 1 Schematic of a single wedge element (left) and four wedge elements arranged to connect two symmetric bricks (right)

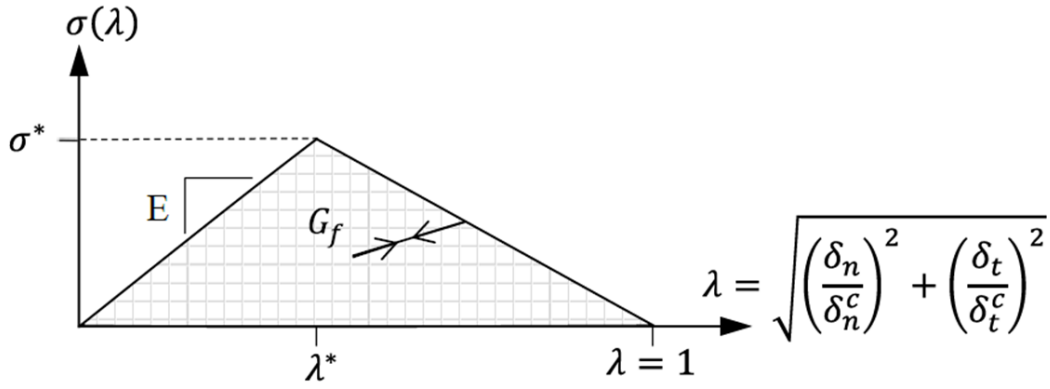

DESCRIPTION CARD FOR COHESIVE MODEL INPUT DATA (2I5,20X,A50)

MATL	11		MATERIAL DESCRIPTION

CARD 2 FOR COHESIVE MODEL INPUT DATA (5F10.0,30X)

DENSITY	DELTANC	DELTATC	DELTAN*	SIGMA*	

Fig. 2 The cohesive material model and input cards required to define its response

The top of Fig. 2 shows the form of the cohesive material model, where the strength, σ, is presented as a function of the normalized separation distance, λ. As the separation increases from zero, the function increases linearly, with a slope denoted by E. After the maximum stress of σ^* is reached at λ^*, the function softens linearly to zero at failure ($\lambda = 1$). Unloading in the softening regime occurs at a reduced slope, so that complete unloading occurs at zero separation. With this form, mixed-mode separation can be modeled using a minimal number of model parameters: δ_n^c and δ_t^c are the normal and tangential single-mode separations at failure, respectively, and $\delta_n^* = \lambda^* \delta_n^c$ and $\sigma^*$are the normal single-mode separation and peak stress, respectively, at the transition from hardening to softening.

The fields on the two lines of input required to define a cohesive material are shown in the lower portion of Fig. 2, where DENSITY is the material density, DELTANC is δ_n^c, DELTATC is δ_t^c, DELTAN* is δ_n^*, and SIGMA* is σ^*. If the density is zero, the cohesive material will make no contributions to the nodal masses. Similarly, if the top and bottom surfaces of a cohesive element are coincident (thickness is zero), then the element will make no contribution to its nodal masses, even if a positive density is provided. A more thorough discussion on the cohesive material model, and its implementation into EPIC, is provided by Beissel[1]; it is also included in the EPIC 2017 beta version user manual.[3]

There are two ways of creating cohesive wedge elements. They can be explicitly meshed using the EPIC input generator or they can be automatically inserted between two joined materials. Each is discussed in turn.

Explicit meshing of cohesive wedge elements is done using a new feature in the EPIC input generator. This new feature allows for a one-element-thick plate, of multiple four-element wedges, to be generated that connects a top and bottom plate comprising symmetric bricks. This approach allows the user to define a desired thickness; this also allows a zero thickness to be used. There are important requirements when using this approach. If a zero thickness is used for the cohesive element, then the virtual-particle option (SEEK = 8 or 18) cannot be used. If a finite thickness is used, then the virtual-particle option can be used (and is the recommended approach), but this requires that the cohesive thickness be at least as large as the radius of a virtual particle, R = DTMAX*VREF, where DTMAX is the maximum time increment allowed and VREF is the reference velocity.

Cohesive wedge elements can also be inserted automatically using a new feature in the EPIC input generator referred to as “cohesive element insertion”. Here the user simply identifies two joined materials (they share nodes at the interface) and cohesive wedge elements are automatically inserted in between the two materials. This option uses the cohesive element insertion card presented in Fig. 3, where MAT1 is the material number for the first joined material, MAT2 is the material number for the second joined material, and MATCO is the material number for the inserted cohesive element. This approach always inserts zero-thickness cohesive elements, thus not allowing the use of the virtual-particle option.

COHESIVE ELEMENT INSERTION CARD (4I5)

18	MAT1	MAT2	MATCO	

Fig. 3 Description of the cohesive element insertion card

Two additional important requirements when using cohesive elements: 1) a contact interface is always required for any computation that includes cohesive elements (automatic sliding is the recommended approach) and MQUAD = 1 must be used and 2) there are no cohesive materials available in the EPIC library, which requires all cohesive materials to be defined in the input file using the two cohesive material model input cards presented in Fig. 2.

3. Results

The following computed results use the new cohesive wedge elements and provide verification that the elements and new features are behaving as expected; they also demonstrate efficiency and robustness. The computed results use the 2017 beta version of the EPIC code.[3]

Figures 4 and 5 compare the computed responses using hexahedral solid and cohesive elements, and tetrahedral (symmetric bricks) and cohesive wedge elements. The results using the hexahedral elements are provided by Beissel[1] and are used to verify the response of the cohesive wedge elements. The cohesive material model constants used are listed in Table 1 and are also provided by Beissel.[1] Figure 4 presents the initial geometry, where the left side uses hexahedral elements and the right side uses symmetric bricks and wedge elements. Figure 5 presents a top-view comparison of cohesive element damage for computations using 0.6- and 0.8-GPa strengths at various times after impact. A significant number of cohesive elements have eroded as there are no elements in the circular center. The results are very similar for both hexahedral and wedge cohesive elements. It should also be noted that several simple computations, using four wedge cohesive elements, were also performed for additional verification.

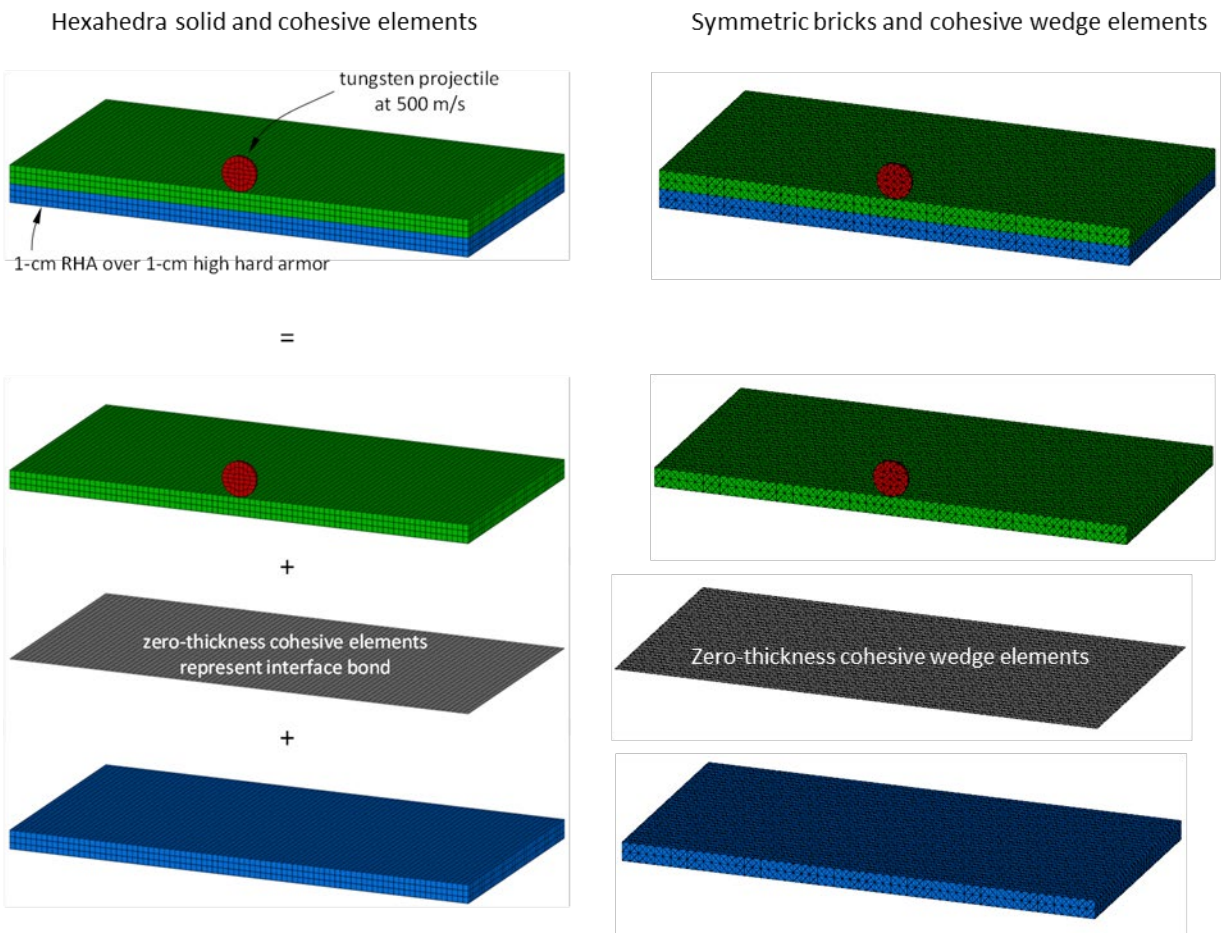

Fig. 4 Initial geometry for a steel sphere impacting a high-hard-steel plate bonded to a rolled homogeneous armor steel plate using cohesive elements. The left side uses hexahedral elements and the right side uses tetrahedral elements.

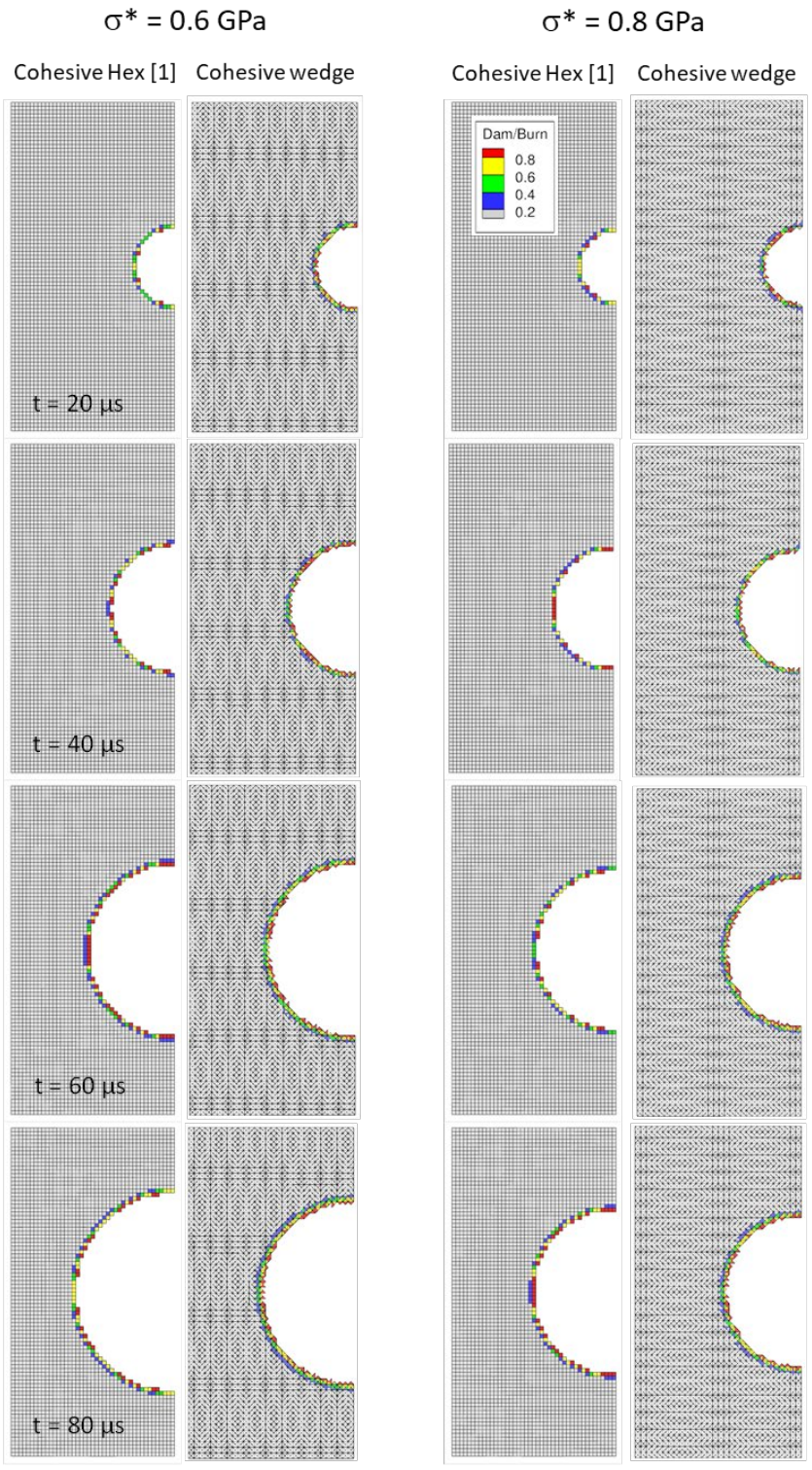

Fig. 5 A comparison of the computed results using cohesive hexahedral elements and cohesive wedge elements. The comparisons are provided for two strengths (σ* = 0.6 and 0.8 GPa) and are shown at t = 20, 40, 60, and 80 μs after impact.

Table 1 Material constants for the cohesive material model characterizing the bond between the two plates

Parameter	Value
δ_n^c	0.1 mm
δ_t^c	0.1 mm
δ_n^*	0.01 mm
σ^*	0.6 GPa, 0.8 GPa

Figure 6 presents a computed result that demonstrates perforation and conversion using cohesive wedge elements. This example computation was run in parallel (distributed), using automatic sliding, and the virtual-particle option (SEEK = 18). The virtual-particle option requires that the thickness, t, of the cohesive elements be no less than the radius, R, of a virtual particle. For this example, R = 0.224 mm and thus the cohesive elements thickness was set to 0.23 mm. Also shown in Fig. 6 are the energies of the projectile, target, and total system as a function of time; they are all well behaved.

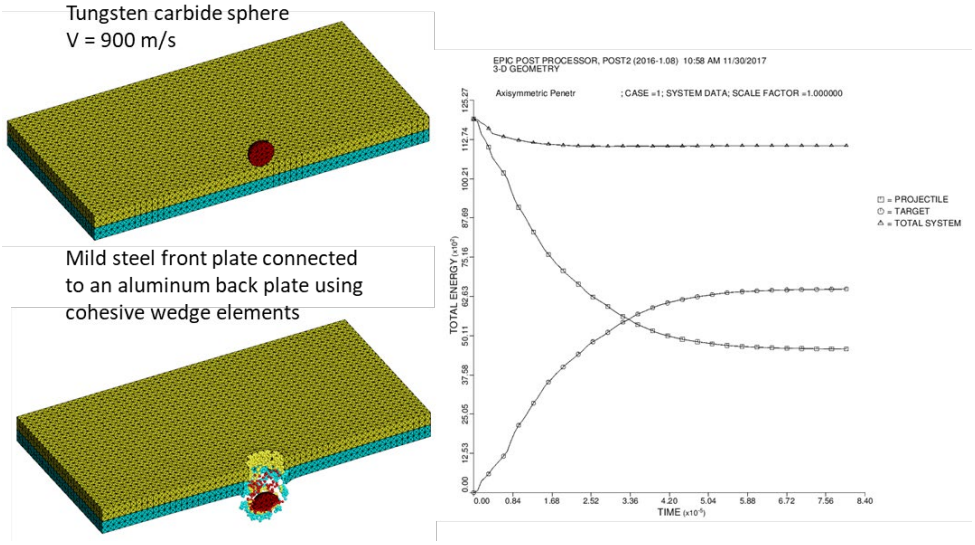

Fig. 6 Computed result for a tungsten carbide sphere impacting a mild steel plate attached to an aluminum back plate using cohesive wedge elements. The sphere perforates the target, and the energies are well behaved.

Lastly, two computations were performed to demonstrate delamination. Figures 7–9 present the results of a steel sphere impacting a plate of Dyneema. Figure 7 presents the initial geometry where a 12.7-mm-diameter steel sphere impacts a 7.9-mm-thick Dyneema plate at 441 or 600 m/s (the initial geometry is provided by Zhang et al.,[4] which also includes experimental results). The Dyneema plate is modeled using four layers of symmetric brick elements, each attached by a

layer of cohesive wedge elements. The symmetric brick elements represent the response of Dyneema using an elastic orthotropic material model that provides for high in-plane strength and low out-of-plane strength. The cohesive wedge elements represent the delamination strength. Figure 8 presents the result for an impact velocity of 441 m/s, where the sphere is stopped in the panel, and Fig. 9 presents the result for an impact velocity of 600 m/s, where the sphere perforates the panel. The computations are robust and efficient, and produce significant delamination.

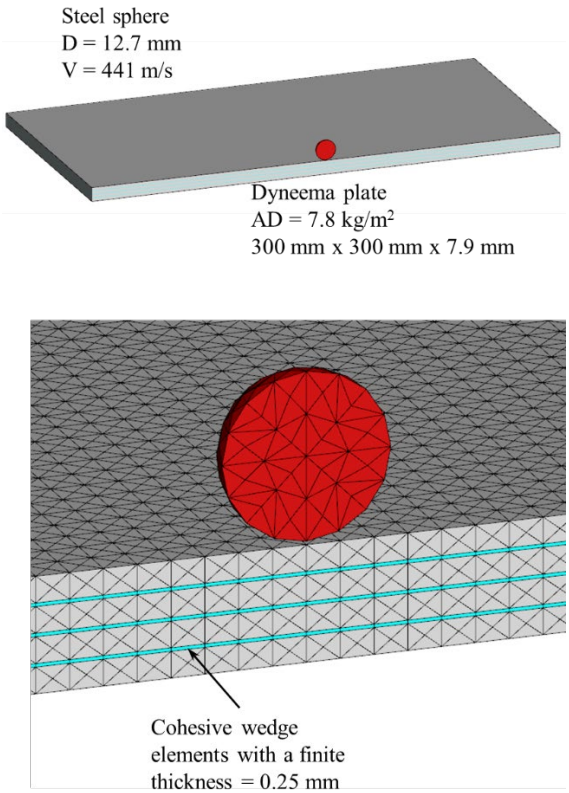

Fig. 7 Initial geometry for a steel sphere impacting a Dyneema panel at 441 or 600 m/s. The panel consists of four symmetric brick layers of Dyneema and are connected using three layers of cohesive wedge elements.

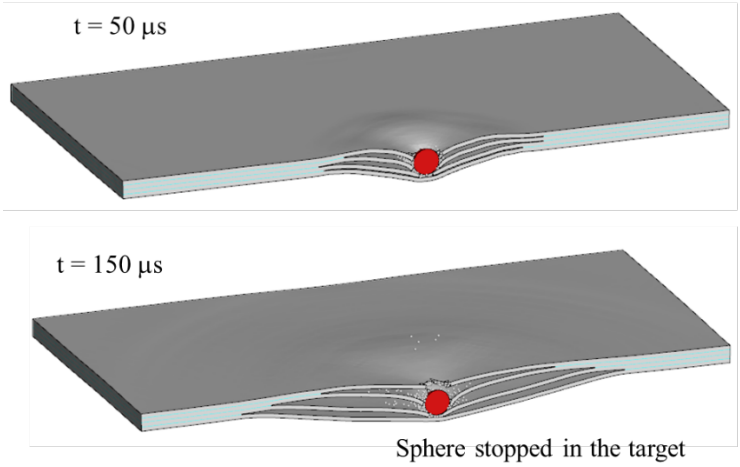

Fig. 8 Computed result for an impact velocity of V = 441 m/s. The sphere is stopped in the target and exhibits severe delamination.

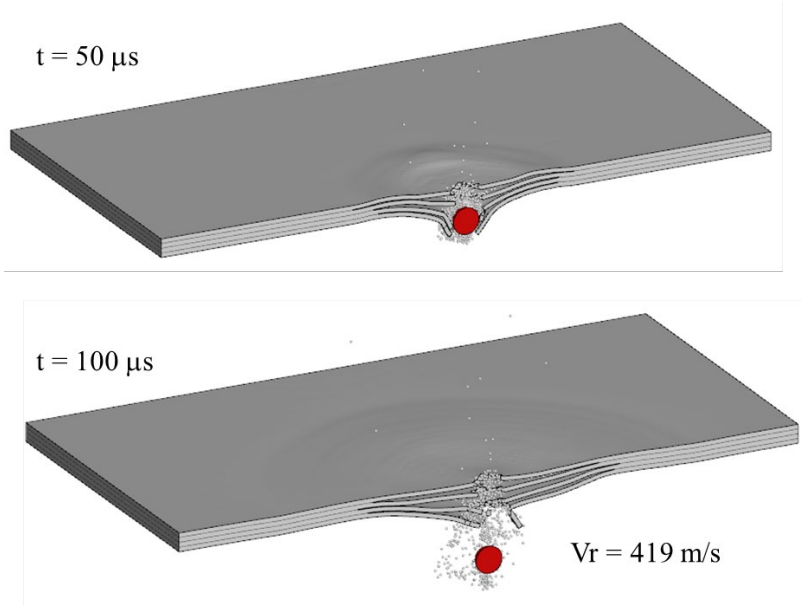

Fig. 9 Computed result for an impact velocity of V = 600 m/s. The sphere perforates the target and exhibits significant delamination.

3. Conclusions

This report documents the incorporation of cohesive wedge elements into the EPIC2017 beta version. The behavior of the cohesive wedge elements was compared to the behavior of cohesive hexahedral elements, and they were in good agreement. Several computations were performed using a sphere to impact various target configurations that included cohesive wedge elements. The computed results demonstrated robustness for configurations that produced severe distortions. The

results also demonstrated that target delamination can be represented using cohesive wedge elements, an important characteristic observed in the Dyneema composite panels. In addition, two methods for creating cohesive wedge elements was also developed. They can be explicitly meshed using the EPIC input generator or they can be automatically inserted between two joined materials.

4. References

1. Beissel SR. The addition of a cohesive model to the EPIC code for simulating interfaces in composite materials. San Antonio (TX): Southwest Research Institute; 2016 Aug. Report No.: 18.19018/017.

2. Gerlach CA, Holmquist TJ. The effect of interface treatment on ceramic performance and modeling Dyneema® subjected to ballistic impact. San Antonio (TX): Southwest Research Institute; 2017 Dec. Report No.: 18.22787.

3. Johnson GR, Beissel SR, Gerlach CA, Holmquist TJ. User instructions for the 2017 beta version of the EPIC code. San Antonio (TX): Southwest Research Institute; 2017 Dec.

4. Zhang TG, Satapathy SS, Vargas-Gonzalez LR, Walsh SM. Ballistic impact response of ultra-high-molecular-weight polyethylene (UHMWPE). Composite Structures. 2015;113.

1 (PDF) DEFENSE TECHNICAL INFORMATION CTR DTIC OCA

1 (PDF) CCDC ARL FCDD RLD CL TECH LIB

1 (PDF) CEERD-GSL K DANIELSON

2 (PDF) CCDC GVSC F RICKERT T TALLADAY

1 (PDF) USAF B PLUNKETT

2 (PDF) AFRL MUNITIONS T SAVAGE K VANDEN

2 (PDF) CCDC AC S RECCHIA

1 (PDF) FUTURES COMMAND D CARLUCCI

4 (PDF) SOUTHWEST RESEARCH INSTITUTE T HOLMQUIST G JOHNSON C GERLACH S BEISSEL

3 (PDF) PEO SOLDIER C BAKER E BEAUDOIN D OTTERSON

4 (PDF) CCDC SC R DILALLA J KIREJCZYK C LEWIS M ROTH

47 (PDF) CCDC ARL FCDD RLC EM J KNAP FCDD RLW S SCHOENFELD A RAWLETT FCDD RLW B C HOPPEL B SCHUSTER R BECKER L VARGAS-GONZALEZ J CAMPBELL P GILLICH A TONGE FCDD RLW L T SHEPPARD FCDD RLW LH D ANDREWS T EHLERS L MAGNESS J NEWILL FCDD RLW M E CHIN FCDD RLW MA E WETZEL T BOGETTI FCDD RLW MB G GAZONAS D HOPKINS B LOVE B POWERS J LIGDA FCDD RLW ME J SWAB J LASALVIA S COLEMAN A DIGIOVANNI FCDD RLW P R FRANCART FCDD RLW PA S BILYK M GREENFIELD FCDD RLW PB S SATAPATHY M SCHEIDLER T WEERASOORIYA J MCDONALD FCDD RLW PC J CAZAMIAS D CASEM J CLAYTON R LEAVY J LLOYD S SEGLETES C WILLIAMS M FERMEN-COKER FCDD RLW PD R DONEY C RANDOW FCDD RLW PE P SWOBODA M LOVE FCDD RLV M M HAILE